BULLETIN OF THE POLISH ACADEMY OF SCIENCES
TECHNICAL SCIENCES, Vol. 69(5), 2021, Article number: e137587
DOI: 10.24425/bpasts.2021.137587

Mechanical alloying of Mg-Zn-Ca-Er alloy

Bartłomiej HRAPKOWICZ [1*], Sabina LESZ [1], Marek KREMZER [1], Małgorzata KAROLUS [2], and Wojciech PAKIEŁA [1]

[1] Department of Engineering Materials and Biomaterials, Silesian University of Technology, ul. Konarskiego 18A, 44-100 Gliwice, Poland
[2] Institute of Materials Engineering, University of Silesia, ul. 75 Pułku Piechoty 1a, 41-500 Chorzów, Poland

Abstract. Magnesium-based materials constitute promising alternatives for medical applications, due to their characteristics, such as good mechanical and biological properties. This opens many possibilities for biodegradable materials to be used as less-invasive options for treatment. Degradation is prompted by their chemical composition and microstructure. Both those aspects can be finely adjusted by means of proper manufacturing processes, such as mechanical alloying (MA). Furthermore, MA allows for alloying elements that would normally be really hard to mix due to their very different properties. Magnesium usually needs various alloying elements, which can further increase its characteristics. Alloying magnesium with rare earth elements is considered to greatly improve the aforementioned properties. Due to that fact, erbium was used as one of the alloying elements, alongside zinc and calcium, to obtain an $Mg_{64}Zn_{30}Ca_4Er_1$ alloy via mechanical alloying. The alloy was milled in the SPEX 8000 Dual Mixer/Mill high energy mill under an argon atmosphere for 8, 13, and 20 hours. It was assessed using X-ray diffraction, energy dispersive spectroscopy and granulometric analysis as well as by studying its hardness. The hardness values reached 232, 250, and 302 HV, respectively, which is closely related to their particle size. Average particle sizes were 15, 16, and 17 μm, respectively.

Key words: magnesium; mechanical alloying; erbium; rare earth elements.

1. INTRODUCTION

Scientific research has always been directed towards improvement of the materials used and their performance [1–3]. Improved properties have been obtained by many different processing techniques, such as chemical, mechanical and laser treatment as well as thermomechanical methods [3–5]. Because of this, ever-increasing demands for improvement have resulted in the development of both advanced materials and methods of their production [6].

Mechanical alloying (MA) is one of the abovementioned methods, which uses the mechanisms of repeated welding, fracturing, and re-welding of powdered particles. It allows for the production of homogeneous materials from a blend of powdered mixtures [1, 7]. It fits very well into the definition of advanced materials, as these are the ones where first consideration is given to the systematic synthesis and control of the structure of the material in order to provide a precisely tailored set of properties for demanding applications [6, 8].

MA allows for "precisely tailored properties" due to the many parameters which can be optimized during the milling process, such as milling time, the milling medium, the ball-to-powder ratio, milling atmosphere, and more. This method usually consists of dry (although it can be wet as well) high-energy ball milling. As MA is one of the solid-state processing methods [9], it allows for the formation of different material classes, such as amorphous alloys, which usually are difficult to obtain by classic methods (i.e. casting) [10, 11]. Furthermore, it is possible to achieve finer microstructure in crystalline as well as nanocrystalline and amorphous alloys [12–20].

Thanks to these qualities, it is possible to obtain specific materials, which would normally be very hard or practically impossible.

That being said, magnesium alloys are one of the most important alloys nowadays. They are lighter while holding their strength. Moreover, they exhibit many beneficial properties such as good mechanical properties and corrosion resistance. The interest in magnesium can be found between many fields of science and industry, such as the automotive or aerospace businesses, and recently its alloys are being considered as potential material for medical application as well. Magnesium alloy based implants, for instance, could be potentially better than their titanium or stainless steel counterparts. Mechanical strength (comparable to that of bone tissue) apart, they offer really good corrosion resistance. As it is known, the human body is a very specific and very corrosive type of environment. Due to that fact, not many materials can be used as implants. Yet when coupled with the MA process, it is possible to prepare highly specialized alloys for any purpose. This is faster, cheaper, and more specialized as compared to more traditional methods [21, 22].

Moreover, magnesium is a very specific material that by itself is not so strong yet highly corrosive. However, when prepared as an alloy with adequate materials, it is possible to achieve the best possible characteristics. In this work, Zn and Ca additions are used to improve both mechanical strength and corrosion resistance [23–28]. To further improve its properties, rare earth elements (REE) can be used [20]. They exhibit some toxicity but can be tolerated to a certain extent. However, they considerably improve the alloy mechanical properties and microstructure in certain cases [29, 30]. Many REEs

*e-mail: bartlomiej.hrapkowicz@polsl.pl

Manuscript submitted 2021-02-26, revised 2021-04-15, initially accepted for publication 2021-05-14, published in October 2021

can be used, as the majority of them increase the mechanical properties, and have higher resistance to *in vivo* degradation [31, 32]. Erbium, as one of the REE is interesting because it was not widely researched in terms of potential uses in biomaterials. The effects of trace erbium additions were investigated in titanium and aluminum alloys. In the case of Mg-Al alloys, erbium addition has improved purity of the alloy, refined the grains, and exhibited more uniform grain distribution. Overall, mechanical properties were improved [33, 34]. Mg-Er alloys were investigated as well, although in larger quantities in terms of atomic composition [32].

The novelty of this paper lies in the new approach to the issue of potential materials for medical applications. Among other materials known from the literature, magnesium-based materials constitute promising alternatives for medical applications, due to their characteristics such as good mechanical and biological properties, corrosion resistance and the reactive ability to interact with other elements. Yet there are not many advanced studies on the influence of Er on the properties of cast magnesium-based alloys in the literature [32–34].

Also, no single study to date reports an influence of Er or the effect of Er on the properties of magnesium-based alloys produced by means of mechanical alloying. Hence the idea was born to conduct the research starting from the basic elements, which is the influence of milling time on the phase composition and microstructure of the material. In this paper, the quaternary Mg-Zn-Ca-Er alloy was investigated as part of a preliminary study to ascertain the effect of high energy milling times on the $Mg_{65}Zn_{30}Ca_4Er_1$ alloy as well as its microstructure and properties. For better clarification, the samples will be represented as $Er_1$8, $Er_1$13 and $Er_1$20, where 8, 13 and 20 is the milling time in an hour.

2. MATERIALS AND METHODS

The powders were processed by mechanical alloying. The nominal composition of the alloy was $Mg_{65}Zn_{30}Ca_4Er_1$. The initial mixture consisted of a mixture of pure powder Mg (99.99% wt.%), Zn (99.99% wt.%) and Er (99.99% wt.%) as well as Ca pellets (99.99% wt.%). The mixture of powders with stainless steel milling balls was closed in stainless steel cylinders under high-purity argon (99.99% wt.%) atmosphere. The ball-to-powder ratio was 10:1.

The processes were carried out on the SPEX 8000D high-energy shaker ball mill at room temperature. The milling consisted of 30 min steps every hour in a shaking mode. The samples were alloyed at a constant frequency with varying milling times of 8, 13, and 20 hours.

The X-ray diffraction (XRD) patterns of studied alloys were measured by using the Empyrean Diffractometer with Cu radiation ($\lambda K_{a1} = 1.5418$ Å) and a PIXcell detector. Phase analyses of substrates and milling products were performed with a High Score Plus PANalytical software integrated with the ICDD PDF4+ 2016 data base while structural studies were done using the Rietveld refinement method integrated with the PANalytical High Score Plus software.

Zeiss 35 scanning electron microscope (SEM), equipped with energy-dispersive spectroscopy (EDS), was used to assess the morphology of the obtained powders. The level of accuracy for EDS of major elements is better than ±2%.

Particle size distribution of the alloy powders was measured using the Fritsch Analysette 22 MicroTec+ in ethyl alcohol.

The hardness test was performed on a Future-Tech FM700 Vickers hardness tester with 15 seconds dwell time and 50 grams of force (HV0.05). The samples were mounted in carbon-based conducting resin, ground and polished. The powder grains were then viewed under microscope in order to select an appropriate grain with sufficient surface area to conduct the microhardness testing.

3. RESULTS AND DISCUSSION

3.1. Phase composition

The comparison of XRD scans obtained for 8, 13 and 20 hours of milling is presented in Fig. 1. The XRD patterns mainly showed the presence of a hexagonal close-packed (HCP) Mg structure (solid state solution) and $MgZn_2$. Moreover, in all milled samples (Fig. 1) the presence of unreacted erbium (Fm3m, cubic structure) has been identified. Structural analysis showed well defined erbium nanocrystallites with values above 500 Å. Crystallite sizes and changes of unit cell parameters of the Mg-based solid state solution and intermetallic $MgZn_2$ phase are presented in Table 1.

Table 1

Crystallite sizes and changes of unit cell parameters of the Mg-based solid state solution and intermetallic $MgZn_2$ phase – main two phases present in alloys after 8, 13 and 20 hours of milling

Sample (milling time)	Mg (Zn, Er, Ca)				$MgZn_2$			
	Theoretical (ICDD PDF4+ card: 04–015–0486)	Refined (RR) a/c [Å]	Crystallite size D [Å]	Lattice strain η [%]	Theoretical (ICDD PDF4+ card: 04–008–7744)	Refined (RR) a/c [Å]	Crystallite size D [Å]	Lattice strain η [%]
8	a = 3.2110 c = 5.2130	3.2066(2) 5.2050(9)	370	0.26	a = 5.2210 c = 8.5670	5.2249(9) 8.5672(8)	300	0.09
13	Space group: $P6_3/mmc$	3.2040(4) 5.1869(3)	300	0.17	Space group: $P6_3/mmc$	5.3406(2) 8. 7977(6)	150	0.37
20	Crystallographic system: hexagonal	3.1853(8) 5.1292(6)	270	0.22	Crystallographic system: hexagonal	5.4855(2) 8.8054(1)	110	0.46

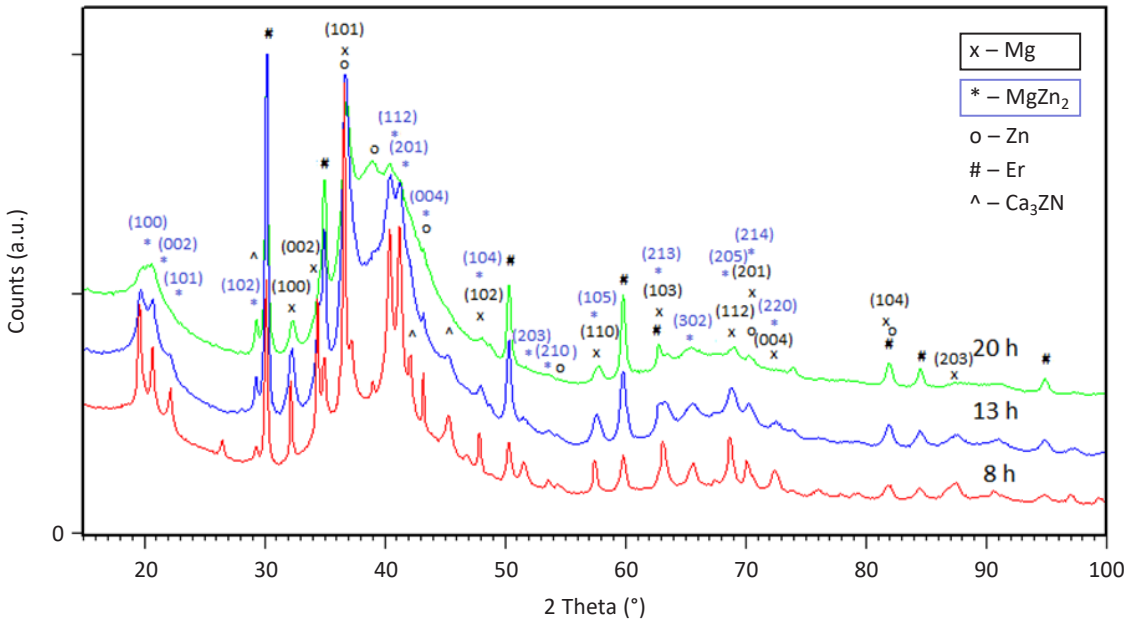

Fig. 1. X-ray diffraction patterns of the Mg-Zn-Ca-Er powders milled for 8, 13 and 20 h

3.2. Granulometry and hardness

The cumulative volume curve distributions and the general volume distribution histograms for Mg-based alloys with varying milling times are presented in Fig. 2a–c for 8, 13, and 20 hours, respectively.

The median value (Q3×50%) for each result was 15, 16, and 17 μm for subsequent samples. The average particle sizes are presented in Table 2, for a clearer representation. It can be seen that the samples are uniformly distributed between ∼10 and ∼60 μm in all cases. In Fig. 2b the smaller peak around

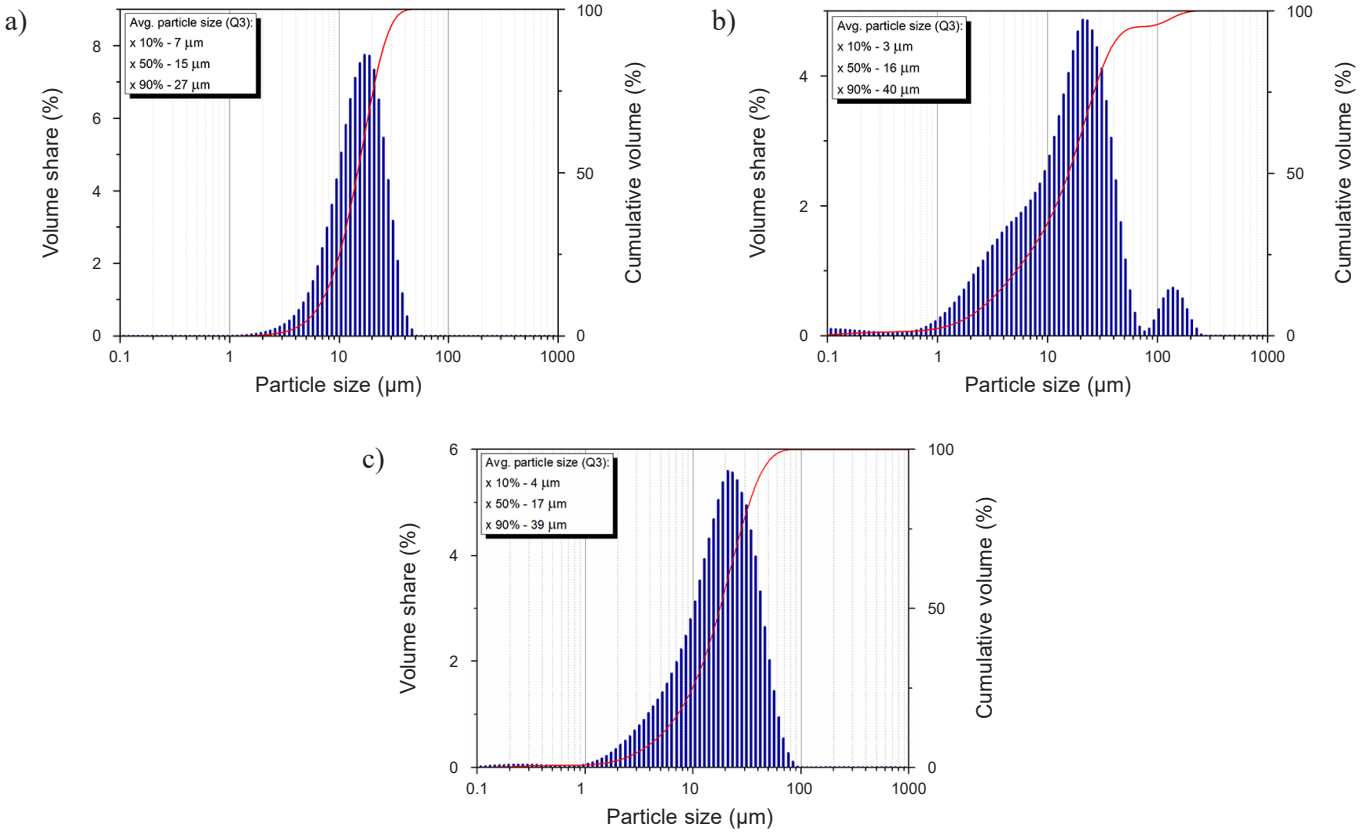

Fig. 2. Particle size volume share (histogram) and their cumulative distribution (curve) for $Mg_{65}Zn_{30}Ca_4Er_1$ alloy milled for a) 8, b) 13 and c) 20 hours

Table 2
Hardness test results and average particle size for samples milled for 8, 13, and 20 hours

Sample	Hardness (HV 0.05)				Avg. particle size [μm]
	Exp. 1	Exp. 2	Exp. 3	Avg.	
$Er_1$8	198	246	253	232 ± 24	15 ± 0.8
$Er_1$13	253	265	233	250 ± 13	16 ± 1.8
$Er_1$20	302	294	309	302 ± 6	17 ± 1

100 μm is caused by particle agglomeration. Although the particles decrease in size during milling, this is due to the finer particle share (Q3×10%) in Fig. 2b–c being larger than after 8 hours in Fig. 2a.

The constant size of the average particle is pointing to the powders being continuously refined, as a result of constant crushing and rewelding [35]. Those claims are supported by the hardness results, which increase with milling time. Average hardness is 232, 250, and 302 HV for samples after 8, 13, and 20 hours, respectively. More detailed results can be seen in Table 2. As the particles change to ultrafine particles, their hardness increases [36].

3.3. Scanning electron microscopy – morphology and qualitative chemical composition analysis

The micrographs representing the powders share many similarities, as seen in Fig. 3.

Visible irregular shapes can be seen along with areas of finer powders. Those irregular shapes are agglomerations caused by the repetitiveness of the mechanical alloying process. As the powder particles constantly clash with each other, they are subjected to welding and fracturing, hence agglomerations occur. The particles may seem larger in Fig. 3a than those in Fig. 3b–c, as opposed to the granulometry results in Fig. 2. But this results from agglomeration and re-welding of the powders, which are later crushed and finish as a finer powder. Moreover, in Fig. 2b the volume share of finer particles is distinctly larger than in Fig. 2a. Hence the difference of sizes of the particles in Fig. 3a and 3b, despite having similar average particle size, as reported in Fig. 2

The results of energy-dispersive spectroscopy are presented in Table 3. The chemical composition is stable after 8 hours of milling and does not vary much from the nominal composition of the powder mixture inserted before milling. This trend continues over 13 and 20 hours (Fig. 4.), meaning that the chemical composition is stable and the only changes occurring are of structural and mechanical nature.

The roundness and uniform distribution of the particles results from longer milling times, as studied by Dobrzański

Table 3
EDS results for samples milled for 8, 13, and 20 hours. The level of accuracy for EDS of major elements is better than ± 2%

Sample	Chemical composition (at.%)			
	Mg	Ca	Zn	Er
$Er_1$8	65.2	4.8	29.2	0.8
$Er_1$13	64.2	4.0	30.6	1.2
$Er_1$20	67.1	3.8	28.1	1.0

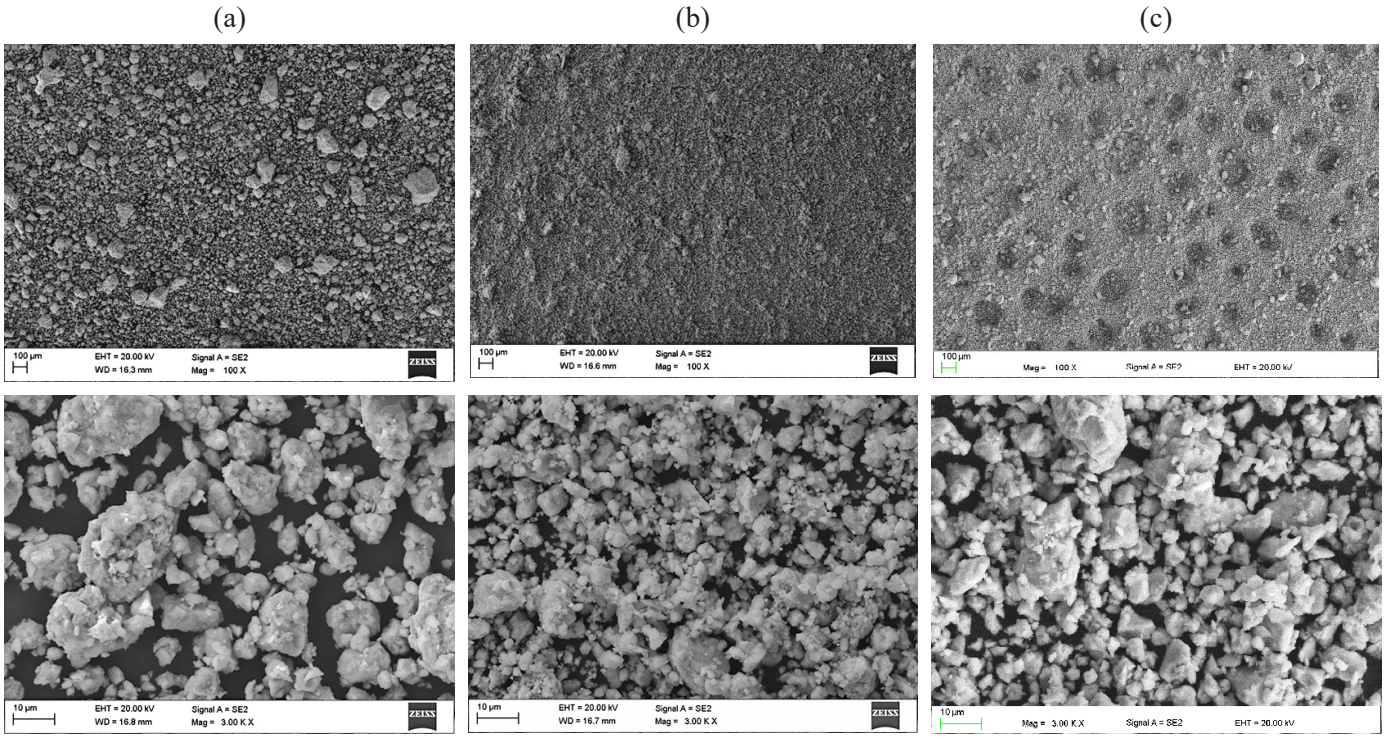

Fig. 3. Selected SEM micrographs showcasing the $Mg_{65}Zn_{30}Ca_4Er_1$ alloy after a) 8, b) 13 and c) 20 hours

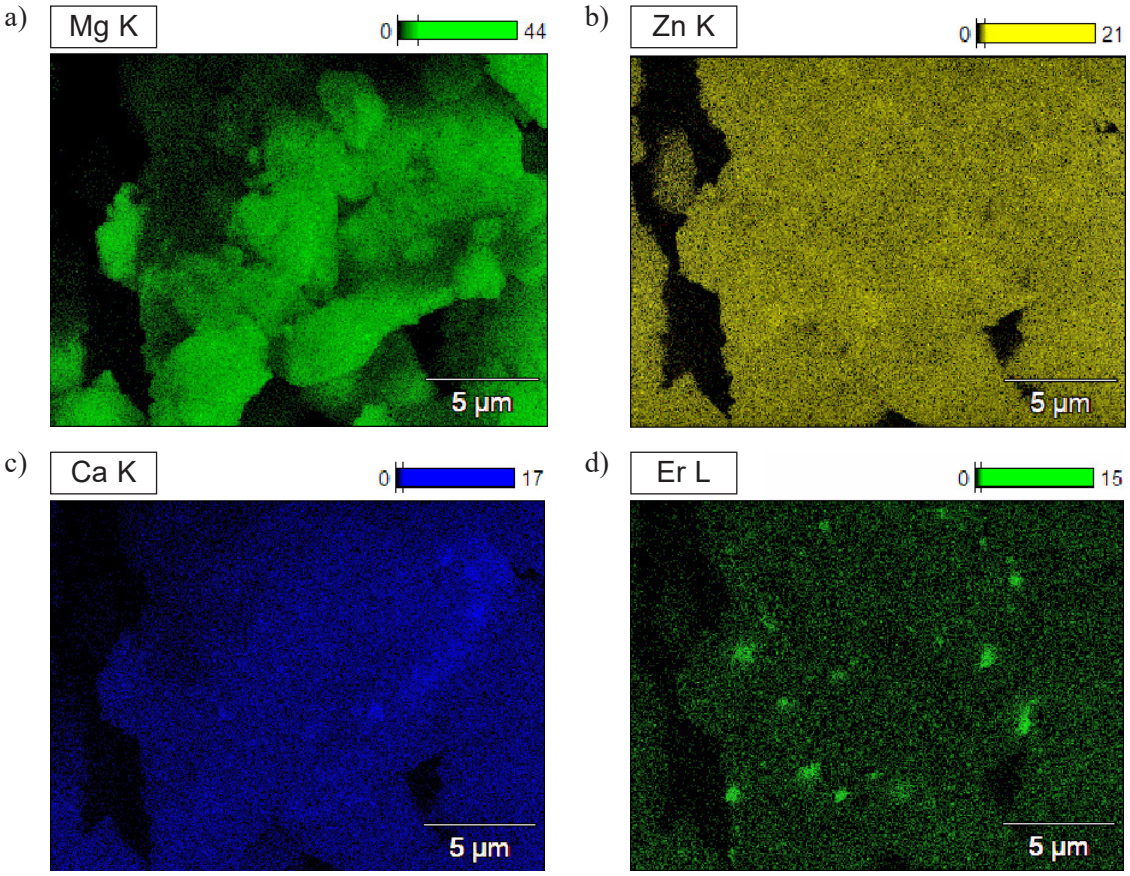

Fig. 4. EDS elemental mapping for $Mg_{65}Zn_{30}Ca_4Er_1$ milled for 20 h visible in Mg (a), Zn (b), Ca (c) and featuring unreacted Er (d)

[37, 38]. This effect can be seen and compared between micrographs in Fig. 3a–c. Moreover, the analysis has confirmed the presence of unreacted, nanocrystalline erbium (~500 nm), which can be seen in Fig. 4d and has been identified in the XRD analysis in Fig. 1. Maps analysis showed a very uniform distribution of unreacted particles in the sample. It was revealed that the unreacted Er is firmly bound to the Mg matrix (Fig. 3, Fig. 4). Areas with an increased atomic share of the remaining structural components of the powder, i.e. Zn (Fig. 4b) and Ca (Fig. 4c), can also be observed.

4. CONCLUSIONS

In order to fully examine how erbium reacts with magnesium alloys during the MA process, it is important to consider the process parameters such as milling time and its influence on the phase composition and microstructure. Those aspects are not commonly discussed in various articles, books and journals that were reviewed in order to gather the data backing up this research. Thus, in order to characterize both physical and chemical properties of the designed material, the following tests were used: X-ray diffraction method, SEM microscopy, particle size distribution by means of granulometric analysis, chemical composition by using energy dispersive spectroscopy and Vickers hardness (HV). Results of those tests were taken into consideration and presented below:

The $Mg_{65}Zn_{30}Ca_4Er_1$ alloy was prepared and milled for 8, 13, and 20 hours. Following this process, the effect of milling times on its morphology, hardness, chemical and phase composition were investigated.

The particles of the milled powders are characterized by sizes between the ranges of 10 to 60 µm, with 15, 16, and 17 µm of average values for 8, 13, and 20 hours of milling time, respectively. Although different, the average values are within the error range, hence it can be said that they are statistically similar. Basing on this statement, it can be concluded that the powders reached the moment of further refining instead of decreasing in size, although the finer particle share increases with milling time.

The Vickers hardness tests yielded results of 232, 250 and 302 HV, showing that hardness increases with milling time. The EDS studies revealed stability of the chemical composition and SEM micrographs show uniform distribution of fine particles. XRD analysis revealed unreacted erbium (Fm3m, cubic structure) in the powder after 20 hours of milling.

As this was a part of a preliminary study, the $Mg_{65}Zn_{30}Ca_4Er_1$ alloy powder will be taken into future consideration for sintering materials.

ACKNOWLEDGEMENTS

This research was funded by the National Science Centre, Poland, grant number 2017/27/B/ST8/02927.

REFERENCES

[1] C. Suryanarayana and N. Al-Aqeeli, "Mechanically alloyed nanocomposites," *Prog. Mater. Sci.*, vol. 58, no. 4, pp. 383–502, May 2013.

[2] C. Suryanarayana, "Mechanical alloying and milling," *Prog. Mater. Sci.*, vol. 46, no. 1–2, pp. 1–184, Jan. 2001.

[3] A. Drygała, L.A. Dobrzański, M. Szindler, M. Prokopiuk Vel Prokopowicz, M. Pawlyta, and K. Lukaszkowicz, "Carbon nanotubes counter electrode for dye-sensitized solar cells application," *Arch. Metall. Mater.*, vol. 61, no. 2A, pp. 803–806, 2016.

[4] L.A. Dobrzański and A. Drygała, "Influence of Laser Processing on Polycrystalline Silicon Surface," *Mater. Sci. Forum*, vol. 706–709, pp. 829–834, Jan. 2012.

[5] L.A. Dobrzański, T. Tański, A.D. Dobrzańska-Danikiewicz, E. Jonda, M. Bonek, and A. Drygała, "Structures, properties and development trends of laser-surface-treated hot-work steels, light metal alloys and polycrystalline silicon," in *Laser Surface Engineering: Processes and Applications*, Elsevier Inc., 2015, pp. 3–32.

[6] C. Suryanarayana, "Mechanical alloying and milling," *Prog. Mater. Sci.*, vol. 46, no. 1–2, pp. 1–184, Jan. 2001.

[7] M. Toozandehjani, K.A. Matori, F. Ostovan, S.A. Aziz, and M.S. Mamat, "Effect of milling time on the microstructure, physical and mechanical properties of Al-Al_2O_3 nanocomposite synthesized by ball milling and powder metallurgy," *Materials (Basel).*, vol. 10, no. 11, p. 1232, 2017.

[8] A. Kennedy *et al.*, "A Definition and Categorization System for Advanced Materials: The Foundation for Risk-Informed Environmental Health and Safety Testing," *Risk Anal.*, vol. 39, no. 8, pp. 1783–1795, 2019.

[9] M. Tulinski and M. Jurczyk, "Nanomaterials Synthesis Methods," in *Metrology and Standardization of Nanotechnology*, Weinheim, Germany: Wiley-VCH Verlag GmbH & Co. KGaA, 2017, pp. 75–98.

[10] K. Cesarz-Andraczke and A. Kazek-Kęsik, "PEO layers on Mg-based metallic glass to control hydrogen evolution rate," *Bull. Polish Acad. Sci. Tech. Sci.*, vol. 68, no. 1, pp. 119–124, 2020.

[11] M. Beniyel, M. Sivapragash, S.C. Vettivel, and P.S. Kumar, "Optimization of tribology parameters of AZ91D magnesium alloy in dry sliding condition using response surface methodology and genetic algorithm," *Bull. Pol. Acad. Sci. Tech. Sci.*, pp. 1–10, 2021.

[12] M. Abbasi, S.A. Sajjadi, and M. Azadbeh, "An investigation on the variations occurring during Ni_3Al powder formation by mechanical alloying technique," *J. Alloys Compd.*, vol. 497, no. 1–2, pp. 171–175, May 2010.

[13] F. Neves, F.M.B. Fernandes, I. Martins, and J.B. Correia, "Parametric optimization of Ti–Ni powder mixtures produced by mechanical alloying," *J. Alloys Compd.*, vol. 509, pp. S271–S274, Jun. 2011.

[14] L. Beaulieu, D. Larcher, R. Dunlap, and J. Dahn, "Nanocomposites in the Sn–Mn–C system produced by mechanical alloying," *J. Alloys Compd.*, vol. 297, no. 1–2, pp. 122–128, Feb. 2000.

[15] J.S. Benjamin and T.E. Volin, "The mechanism of mechanical alloying," *Metall. Trans.*, vol. 5, pp. 1929–1934, 1974.

[16] S. Lesz, J. Kraczla, and R. Nowosielski, "Structure and compression strength characteristics of the sintered Mg–Zn–Ca–Gd alloy for medical applications," *Arch. Civ. Mech. Eng.*, vol. 18, no. 4, pp. 1288–1299, Sep. 2018.

[17] S. Lesz, B. Hrapkowicz, M. Karolus, and K. Gołombek, "Characteristics of the Mg-Zn-Ca-Gd alloy after mechanical alloying," *Materials (Basel).*, vol. 14, no. 1, pp. 1–14, 2021.

[18] S. Lesz, T. Tański, B. Hrapkowicz, M. Karolus, J. Popis, and K. Wiechniak, "Characterisation of Mg-Zn-Ca-Y powders manufactured by mechanical milling," *J. Achiev. Mater. Manuf. Eng.*, vol. 103, no. 2, pp. 49–59, 2020.

[19] M. Karolus and J. Panek, "Nanostructured Ni-Ti alloys obtained by mechanical synthesis and heat treatment," *J. Alloys Compd.*, vol. 658, pp. 709–715, Feb. 2016.

[20] A. Chrobak, V. Nosenko, G. Haneczok, L. Boichyshyn, M. Karolus, and B. Kotur, "Influence of rare earth elements on crystallization of Fe 82Nb2B14RE2 (RE = Y, Gd, Tb, and Dy) amorphous alloys," *J. Non. Cryst. Solids*, vol. 357, no. 1, pp. 4–9, Jan. 2011.

[21] B. Hrapkowicz and S.T. Lesz, "Characterization of Ca 50 Mg 20 Zn 12 Cu 18 Alloy," *Arch. Foundry Eng.*, vol. 19, no. 1, pp. 75–82, 2019.

[22] M.K. Datta *et al.*, "Structure and thermal stability of biodegradable Mg–Zn–Ca based amorphous alloys synthesized by mechanical alloying," *Mater. Sci. Eng. B*, vol. 176, no. 20, pp. 1637–1643, Dec. 2011.

[23] J. Zhang *et al.*, "The degradation and transport mechanism of a Mg-Nd-Zn-Zr stent in rabbit common carotid artery: A 20-month study," *Acta Biomater.*, vol. 69, pp. 372–384, 2018.

[24] M. Yuasa, M. Hayashi, M. Mabuchi, and Y. Chino, "Improved plastic anisotropy of Mg–Zn–Ca alloys exhibiting high-stretch formability: A first-principles study," *Acta Mater.*, vol. 65, pp. 207–214, Feb. 2014.

[25] L.M. Plum, L. Rink, and H. Haase, "The essential toxin: impact of zinc on human health.," *Int. J. Environ. Res. Public Health*, vol. 7, no. 4, pp. 1342–65, 2010.

[26] M. Salahshoor and Y. Guo, "Biodegradable Orthopedic Magnesium-Calcium (MgCa) Alloys, Processing, and Corrosion Performance.," *Mater. (Basel, Switzerland)*, vol. 5, no. 1, pp. 135–155, Jan. 2012.

[27] H.S. Brar, M.O. Platt, M. Sarntinoranont, P.I. Martin, and M.V. Manuel, "Magnesium as a biodegradable and bioabsorbable material for medical implants," *Jom*, vol. 61, no. 9. pp. 31–34, 2009.

[28] M. Pogorielov, E. Husak, A. Solodivnik, and S. Zhdanov, "Magnesium-based biodegradable alloys: Degradation, application, and alloying elements," *Interventional Medicine and Applied Science*, vol. 9, no. 1. pp. 27–38, 2017.

[29] N. Hort *et al.*, "Magnesium alloys as implant materials – Principles of property design for Mg–RE alloys," *Acta Biomater.*, vol. 6, no. 5, pp. 1714–1725, May 2010.

[30] Y. Kawamura and M. Yamasaki, "Formation and mechanical properties of $Mg_{97}Zn_1RE_2$ alloys with long-period stacking ordered structure," *Mater. Trans.*, vol. 48, no. 11, pp. 2986–2992, 2007.

[31] C. Liu, Z. Ren, Y. Xu, S. Pang, X. Zhao, and Y. Zhao, "Biodegradable Magnesium Alloys Developed as Bone Repair Materials: A Review," *Scanning*, vol. 2018. p. 9216314, 2018.

[32] S. Seetharaman, S. Tekumalla, B. Lalwani, H. Patel, N.Q. Bau, and M. Gupta, "Microstructure and Mechanical Properties New Magnesium-Zinc-Gadolinium Alloys," in *Magnesium Technology 2016*, Cham: Springer International Publishing, 2016, pp. 159–163.

[33] S. Seetharaman *et al.*, "Effect of erbium modification on the microstructure, mechanical and corrosion characteristics of binary Mg-Al alloys," *J. Alloys Compd.*, vol. 648, pp. 759–770, Jul. 2015.

[34] R. Ahmad, N.A. Wahab, S. Hasan, Z. Harun, M.M. Rahman, and N.R. Shahizan, "Effect of erbium addition on the microstructure and mechanical properties of aluminium alloy," in *Key Engineering Materials*, 2019, vol. 796, pp. 62–66.

[35] C.L. Chen and Y.M. Dong, "Effect of mechanical alloying and consolidation process on microstructure and hardness of nano-structured Fe-Cr-Al ODS alloys," *Mater. Sci. Eng. A*, vol. 528, no. 29–30, pp. 8374–8380, Nov. 2011.

[36] K. Kowalski, M. Nowak, J. Jakubowicz, and M. Jurczyk, "The Effects of Hydroxyapatite Addition on the Properties of the Mechanically Alloyed and Sintered Mg-RE-Zr Alloy," *J. Mater. Eng. Perform.*, vol. 25, no. 10, pp. 4469–4477, Oct. 2016.

[37] L.A. Dobrzański, B. Tomiczek, G. Matula, and K. Gołombek, "Role of Halloysite Nanoparticles and Milling Time on the Synthesis of AA 6061 Aluminium Matrix Composites," *Adv. Mater. Res.*, vol. 939, pp. 84–89, May 2014.

[38] J. Dutkiewicz, S. Schlueter, and W. Maziarz, "Effect of mechanical alloying on structure and hardness of TiAl-V powders," in *Journal of Metastable and Nanocrystalline Materials*, 2004, vol. 20–21, pp. 127–132.